JBUON 2019; 24(6): 2380-2387
ISSN: 1107-0625, online ISSN: 2241-6293 • www.jbuon.com
Email: editorial_office@jbuon.com

ORIGINAL ARTICLE

Association of LncRNA-GACAT3 with MRI features of breast cancer and its molecular mechanism

Haifeng Hu[1]*, Ying Wang[2]*, Tianyu Zhang[3], Chunyu Zhang[1], Ying Liu[1], Guoan Li[1], Dandan Zhou[2], Shengnan Lu[2]

[1]Department of MRI, the second Affiliated Hospital of Qiqihar Medical University, Qiqihar 161006, P.R. China; [2]Department of Ultrasound, the second Affiliated Hospital of Qiqihar Medical University, Qiqihar 161006, P.R. China; [3]Department of CT, the second Affiliated Hospital of Qiqihar Medical University, Qiqihar 161006, P.R. China.

*Haifeng Hu and Ying Wang contributed equally to this study.

Summary

Purpose: *This study was designed to investigate the relationship between the abnormal expression of LncRNA GACAT3 and the prognosis of breast cancer patients, preoperative magnetic resonance imaging (MRI) parameters and the molecular downstream mechanism.*

Methods: *Quantitative fluorescence PCR was used to detect the expression of LCCRNA GACAT3 in 20 breast cancer tissues and adjacent tissues. Patients were divided into low expression group and high expression group according to the level of expression, and the differences and overall survival of MRI diffusion-weighted imaging parameters were analyzed. The expression of LCCRNA GACAT3 was interfered by MCV-7 cells transfected by recombinant adenovirus, and the proliferation and apoptosis of MCF-7 were detected by BrdU method and TUNEL method, respectively.*

Results: *The expression of LncRNA GACAT3 was increased in breast cancer tissues and cell lines compared to paracancer tissues and normal cells. Compared with the low expression group, patients with high expression had poorer MRI diffusionweighted imaging and lower overall survival. Down-regulation of LncRNA GACAT3 increased the expression of miR-497, and miR-497 mimics reduced the luciferase of LncRNA GACAT3. Increased LrcRNA GACAT3 in breast cancer cells could downregulate the expression of miR-497, down-regulate Capsase 9 and up-regulate Bcl-2 to promote proliferation and anti-apoptosis of breast cancer cells.*

Conclusion: *LncRNA GAC AT3 is associated with poor prognosis of breast cancer, preoperative MRI perfusion-related diffusion (D) reduction, and elevated perfusion fraction (f). After targeting CIR-497, LncRNA GACAT3 promotes the progression of breast cancer by down-regulating Caspase 9 and up-regulating Bcl-2.*

Key words: *lncRNA, breast cancer, magnetic resonance imaging, proliferation, apoptosis*

Introduction

Breast cancer is the most common malignant tumor in women, and its incidence has always ranked first in women's cancers [1,2]. In the past few decades, breast cancer-related mortality has declined due to significant advances in testing, diagnosis, and treatment [3]. However, the side effects of treatments limit the treatment of breast cancer [4]. Therefore, it is very important to understand the pathogenesis of breast cancer and to find out new therapeutic targets of breast cancer to improve the treatment of breast cancer and the prognosis of patients.

Magnetic resonance imaging (MRI) has been considered superior to physical examination, mammography or ultrasound in preoperative evaluation of breast cancer [5,6]. Currently, MRI based on contrast-enhanced residual tumor size and volume

Corresponding author: Dr. Haifeng Hu, MM. Department of MRI, the second Affiliated Hospital of Qiqihar Medical University, No.37 Zhonghua West Rd, Jianhua District, Qiqihar 161006, P.R. China
Tel/Fax: + 86 17382826981, Email: huhaifeng0419@126.com
Received: 09/06/2019; Accepted: 13/07/2019

is commonly used as an indicator of preoperative tumor size and infiltration [7,8]. Diffusion-weighted imaging (DWI) is considered a potential method to overcome traditional MRI assessments that are limited to intrinsic special tissues [9]. For the first time, Le Bihan et al proposed the Intravoxel Incoherent Motion (IVIM) theory based on DWI to obtain perfusion-related diffusion associated with perfusion (D) and perfusion fraction (f) in tissues without the application of contrast agents [9]. This IVIM method has been shown to be useful in distinguishing between benign and malignant biological behavioral features of tumors, and even predictive efficacy of postoperative adjuvant chemotherapy [10-12]. This type of discrimination is clearly based on the responsiveness of perfusion-related diffusion (D) and perfusion fraction (f) to the degree of angiogenesis in the tumor.

Human transcriptome studies have found that most RNAs are not translated after transcription [13]. The long non-coding RNA (lncRNA) is a non-coding RNA comprising more than 200 nucleotides. LncRNA triggers endogenous RNA interference and is involved in post-transcriptional regulation, and its aberrant expression plays an important regulatory role in the development of many types of tumors [14,15]. LncRNA inhibits the normal function of the target nucleotide by binding to the target miRNA, thereby regulating the regulation of cell proliferation, apoptosis, differentiation and drug resistance. Emerging evidence suggests that lncRNAs play a crucial role in the development and progression of cancer [16,17]. The lncRNA AC130710 was named gastric cancer-associated transcript 3 (GACAT3) [18]. LncRNA GACAT3 has been found to increase in gastric cancer and is involved in tumor proliferation and lymph node metastasis by negatively regulating miR-497 expression [19-22]. However, few studies have reported the potential regulatory role of lncRNA GACAT3 in breast cancer and its association with perfusion-related diffusion (D) and perfusion fraction (f) and other important tools for preoperative tumor evaluation. Therefore, the aim of this study was to investigate the expression of lncRNA GACAT3 in breast cancer, and to explore the relationship between the high and low expression of lncRNA GACAT3 and the prognosis of patients, preoperative MRI parameters, and the underlying biological mechanisms.

Methods

Material

Participants: The cancer and adjacent cancer tissues from women with breast cancer who underwent surgery and MRI in our hospital from June 2016 to July 2017 were collected.

Inclusion criteria: patients aged 23-76 years; all were subjected to core needle biopsy to confirm the presence of tissue invasive breast cancer; the distance between the edge of the cancer tissue and the adjacent to cancer tissue was about 2 cm; breast conserving surgery, axillary lymph node dissection or modified radical mastectomy; first diagnosis; surgical resection including R0 (no cancer cells within 1 mm of all resection margins) or R1 (cancer cells present within 1 mm of one or more resection margins); peripheral whole blood exams normal; liver and renal functions normal. *Exclusion criteria:* non-mammary invasive ductal carcinoma; incomplete (R2) resection; previous chemotherapy or radiotherapy; distant metastasis, malignant ascites or pleural effusion; anemia, thrombocytopenia; serum total bilirubin level ≥ 1.5 times the upper limit of normal, creatinine clearance ≤ 50 ml per min; patients with symptomatic heart failure or coronary heart disease; DWI images difficult to assess due to obvious artifacts; pregnancy or any MRI contraindications (including metal implants, cardiac pacemakers, cardiac metal stents); and allergic reactions to MRI contrast agents.

Finally, 20 cases were collected, aged 43.96±9.79 years old. A portion of the surgically removed specimen was immediately stored in a centrifuge tube without RNase and stored in a refrigerator at -80 °C. The study was approved by the ethics committee and all subjects signed the informed consent form.

Cell lines, adenoviral vectors and primers: normal breast cell line MCF-10A and breast cancer cell lines MCF-7 and HEK293T were obtained from Shanghai Institute of Biological Sciences, Chinese Academy of Sciences. HEK293T was cultured in DMEM, and MCF10A was cultured in a 1:1 mixed medium of F12/DMEM 77. MCF7 was cultured in MEM medium containing sodium pyruvate 0.11 mg/ml and bovine insulin 0.01 mg/ml. All cells were cultured in medium containing 10% fetal bovine serum (FBS; Gibco, Grand Island, NY, USA), 100 U/ml penicillin and 100 mg/ml streptomycin (Gibco, Grand Island, NY, USA). The culture conditions were 37°C and 5% CO_2. Lentiviral vectors carrying shNC, shGACAT3, NC and GACAT3 and miR497 mimics and inhibitors and their respective negative control RNAs were obtained from GeneBio Company (Shanghai, China). Specific shRNA expression plasmid pLKO-shSRC-3, targeting sequence 5'-TTCCACCTCCTAGGGATATAA-3'; GACAT3 upstream primer: 5'-CTTCCGGAGCAGGTCTGAGT-3', downstream primer: 5'-CTTTCCCTGCAGAGACCAGT-3'; miR-497 upstream Primer: 5'AGTCCAGTTTTCCCAGGAATCCCT-3', downstream primer: 5'ACCAGCAGCACACTGTGGTTTGT-3'; GAPDH upstream primer: 5'-GTCAACGGATTTGGTCTGTATT-3', downstream primer: 5'-AGTCTTCTGGGTGGCAGTGAT-3', all purchased from Sigma-Aldrich.

Main reagents: reverse transcription kit iScript reverse transcription supermix (item number: 1708841), real-time quantitative PCR reaction kit SYBR® Premix Ex Taq™ II (TliRNaseH Plus) (item number: RR820A) was purchased from takara. RIPA lysate (item No. P0013B) was purchased from Biotime Biotechnology Co., Ltd. Fetal bovine serum (item No. 10438026), BCA protein assay kit (item No. 23235), PVDF membrane (item No. LC2005) were purchased from ThermoFisher Scientific.

Dulbecco's modified Eagle medium (DMEM) dry powder (Item. No. D5030), MTT (item No. D5655) was purchased from Sigma. EDTA-trypsin (item No. 0785) was purchased from Amresco.

Instruments: Fluorescence quantitative PCR instrument was Roche Lightcycler 480 Quantitative Analysis System (Applied Biosystems), nucleic acid analyzer was Nanodrop2000, MRI instrument was PHILIPS-Achieva 1.5T.

Magnetic resonance imaging

Whole-body MRI was performed. All patients were imaged in the prone position using an 8-channel phased array breast coil. Patients were fasted for at least 2 hours prior to imaging and avoided any strenuous exercise prior to examination.

Conventional MR breast imaging included lateral T2-weighted imaging fat suppression, lateral DWI fat suppression, short-term inversion recovery (STIR) (b=0,1000 s/mm^2), lateral 3D Vibrant-Flex multiphase dynamic contrast enhancement (DCE-MRI) and sagittal 3D Vibrant-Flex was used for delayed acquisition. Transverse multi-b DWI was obtained prior to DCE-MRI using STIR fat saturated single spin echo planar imaging (SE-EPI). Twelve b values were used: 0, 10, 20, 30, 50, 70, 100, 150, 200, 400, 800 and 1000 s/mm^2. The number of excitations (NEX) was 1, 3, 3, 3, 3, 2, 2, 2, 2, 3, 5, and 6, respectively. The corresponding parameters were as follows: repeat time/echo time: 2400/62.1 ms; field of view: 320×320 mm; matrix size: 128×160; section thickness: 5 mm; cross gap: 1 mm; flip angle: 90°; Receiver bandwidth: 250 kHz; parallel imaging (ASSET) factor: 2. The imaging duration of the multi-b DWI sequence was 8 min and 19 s. For the DCE-MRI sequence, the lateral 3D Vibrant-Flex scanning was performed and repeated 9 times (each for 45 s) before intravenous administration of 0.1 mmol/kg Gd-DTPA (Magnevist; Bayer, Berlin, Germany) at 2 mL/s (a power injector with 15 s time delay was used, then rinsed with 20 ml of saline).

1. Relative expression of lncRNAGACAT3 and miR-497 in breast cancer, adjacent tissues and cell lines: 1 g of fresh tissue blocks were taken and total RNA was extracted by Trizol method. A nucleic acid analyzer was used to detect purity, concentration, and impurities. The first strand cDNA was then synthesized by a reverse transcription kit. The reaction system: cDNA 2 ul, SYBR® Premix Ex Taq™ II (2×) 10 ul, upstream and downstream primers (10 uM) each 0.4ul, ROX 0.4ul, H_2O6.8ul. PCR was performed in a real-time quantitative fluorescent PCR instrument (ABI 7300, USA). The PCR conditions were 95°C for 30 s and 95°C for 15 s. The 3-phosphate dehydrogenase (GAPDH) gene was used as an internal reference to analyze relative gene expression levels using the $2^{-\Delta\Delta CT}$ method.

2. MCF-7 transfection: MCF-7 cells were cultured in a 24-well plate at a concentration of 1×10^5 cells/ml. When reached 60% confluence, recombinant adenovirus was added, 1 ul/well, cultured in 37°C, 5% CO_2 incubator overnight, the virus transfection efficiency was observed under a fluorescence microscope, and MCF-7 cells were transfected into an empty vector as a control.

3. Cell Proliferation Capability Assay: Proliferation was assessed by measuring 5-BrdU incorporation to assess DNA synthesis. The cells were seeded at a density of 2×10^3 cells/well in 96-well culture plates, cultured for 24-72 h, and then cultured at a final concentration of 10 mM BrdU (BD Pharmingen, CA, USA). After 2 h of incubation, the medium was removed, the cells were fixed at room temperature for 30 min, and incubated with peroxidase-conjugated anti-BrdU antibody (Sigma-Aldrich, USA) (working concentration 1:1000) at room temperature for 60 min. The cells were then washed three times with PBS and incubated with peroxidase substrate (tetramethylbenzidine) for 30 min. Finally, the absorbance at 450 nM was measured using a microplate reader (Thermo Fisher Scienific, IL, USA). The relative number of 1-3 days was calculated by continuously monitoring for 3 days based on the number of cells on day 0. Three separate experiments were performed.

4. Measurement of apoptosis: Apoptotic cell death was assessed using the TdTmediated dUTP nick end labeling (TUNEL) fluorescent FITC kit (Roche, Basel, Switzerland). After treatment, cells were fixed with 4% paraformaldehyde and permeabilized in 0.1% Triton X-100. Then, the cells were incubated with TUNEL in an incubator at 37°C for 1 h. After washing twice with PBS, FITC fluorescence was analyzed using a cell counter (BD Biosciences, USA). Results were expressed as the percentage of apoptotic cells compared to the control.

5. Luciferase activity assay: HEK293T cells were seeded at 1.5×10^4/well in 96-well plates and co-expressed with 200 ng GACAT3-WT, GACAT3-MUT, CCND2-WT or CCND2-MUT (Sangon Biotech, China). HEK293T cells were also co-transfected with 10 ng of pRL-TK (Promega, USA) and miR-497 mimic or miRNA NC using Lipofectamine 2000 (Invitrogen, Carlsbad, CA, USA). Luciferase assays were determined 48 h after transfection using a dual luciferase reporter assay system (Promega, USA).

Statistics

Statistical analyses were performed using SPSS 22.0 statistical software. The Kolmogorov-Smirnov test was used to estimate the distribution of all parameters: normal distribution data was expressed as mean ± standard deviation, while non-normal data was expressed as median and quartile ranges. Differences in parameters (D, D*, f, MD, and V) before NAC and after 2 cycles of NAC between non-pCR and pCR groups were compared using Student's t-test or non-parametric test. Three independent experiments were performed for each experiment. Kaplan-Meier and log-rank test were used to analyze and compare the relationship between GCAT3 level and prognosis of breast cancer patients. The difference was statistically significant at $p< 0.05$.

Results

Up-regulation of LncRNA GACAT3 is associated with poor prognosis of breast cancer patients, decreased D value of magnetic resonance imaging parameters, and increased F value

The expression of LncRNA GACAT3 was significantly increased in breast cancer tissues compared

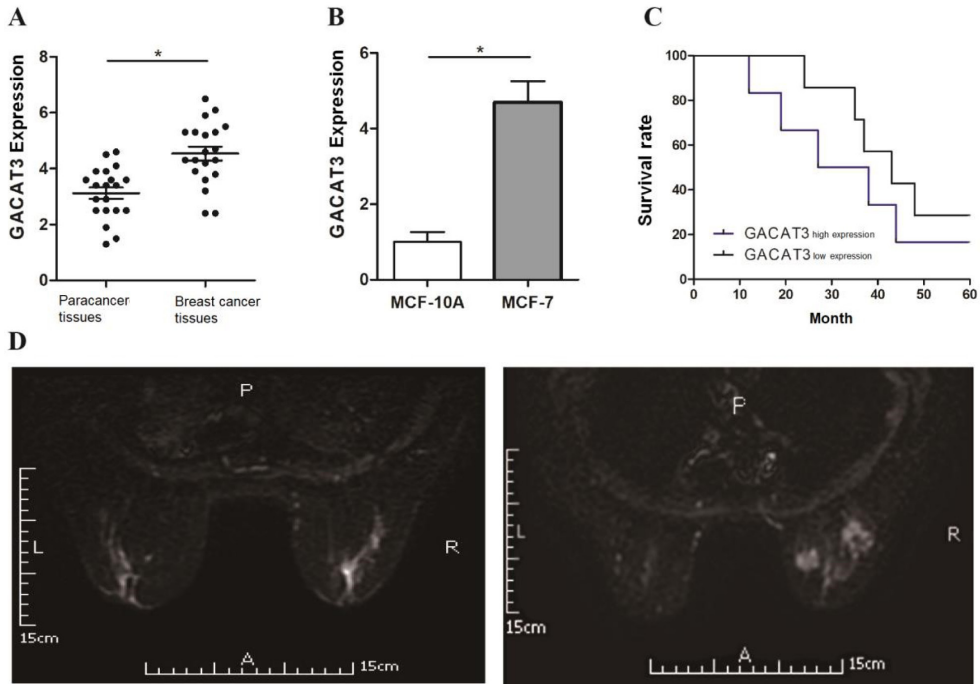

Figure 1. Correlation of up-regulation of LncRNA GACAT3 with MRI features and prognosis in breast cancer patients. **A:** LncRNAGACAT3 expression in paracancer tissues and breast cancer tissues measured by qRT-PCR. **B:** LncRNAGACAT3 expression in normal breast cells and breast cancer cell lines measured by qRT-PCR. **C:** Breast cancer patients were divided into GACAT3 high expression group and low expression group, and Kaplan-Meier analysis was used to analyze the relationship between GACAT3 expression level and prognosis of breast cancer patients. **D:** Typical MRI diffusion-weighted imaging of patients with lower LncRNA GACAT3 expression (left panel) and higher expression (right panel). *P<0.05 compared to the control.

Table 1. Comparison of diffusion-weighted imaging parameters between groups of high and low LCCRNA GACAT3 expression levels

DWI parameter	*LncRNA GACAT3 expression Number*		*p value*
	Low (10)	*High (10)*	
D(*10^{-3}mm^2/s)	1.30 ± 0.21	0.92 ± 0.18	0.000*
D*(*10^{-3}mm^2/s)			0.587
Median number	10.76	11.30	
Range	4.98-29.65	3.27-33.42	
F (%)			0.000*
Median number	21.76	31.05	
Range	15.67-23.76	20.67-37.48	

D*: perfusion-related diffusion coefficient; D: true molecular diffusion coefficient; f: perfusion fraction; IVIM: intravoxel incoherent motion. Normal distribution data were expressed as mean±standard deviation, such as true molecular diffusion coefficient. Non-normal data were expressed as median and quartile ranges, such as perfusion-related diffusion coefficients, perfusion scores.

with adjacent tissues, and there was a statistical difference (p=0.034) (Figure 1A). Furthermore, the expression of LncRNA GACAT3 was significantly increased in the breast cancer cell line MCF-7 compared to the normal breast cell line MCF-10A (Figure 1B). For patients with higher expression of LncRNA GACAT3, MRI diffusion-weighted imaging (DWI) parameter D values (0.92±0.18) were lower than those with lower expression of LCCRNA GACAT3 (1.30±0.21, p=0.0008), F values were higher (median number 31.05 vs. 21.76, p=0.0004) (Figure 1C), overall survival time was lower (Figure 1D), all with statistical differences (Table 1).

miR-497 is the target of LncRNA GACAT3 in the regulation of breast cancer cell proliferation

Knockdown of LncRNA GACAT3 inhibited MCF-7 cell proliferation (Figure 2A), whereas overexpression of LncRNA GACAT3 promoted MCF-7 cell proliferation (Figure 2B). Bioinformatics predicted that miR-497 was a potential target for LncRNA GACAT3 to regulate tumor cell proliferation and invasion in breast cancer (Figure 2C). Correlation regression showed that the expression level of miR-497 was negatively correlated with LncRNA GACAT3 in tumor tissues (Figure 2D). Overexpression of LncRNA GACAT3 significantly inhibited miR-497 levels in MCF-7 cells (Figure 2E), whereas knockdown of LncRNA GACAT3 significantly upregulated miR-497 expression (Figure 2F). Luciferase reporter assay showed that LRCRNA GACAT3 WT luciferase activity decreased signifi-

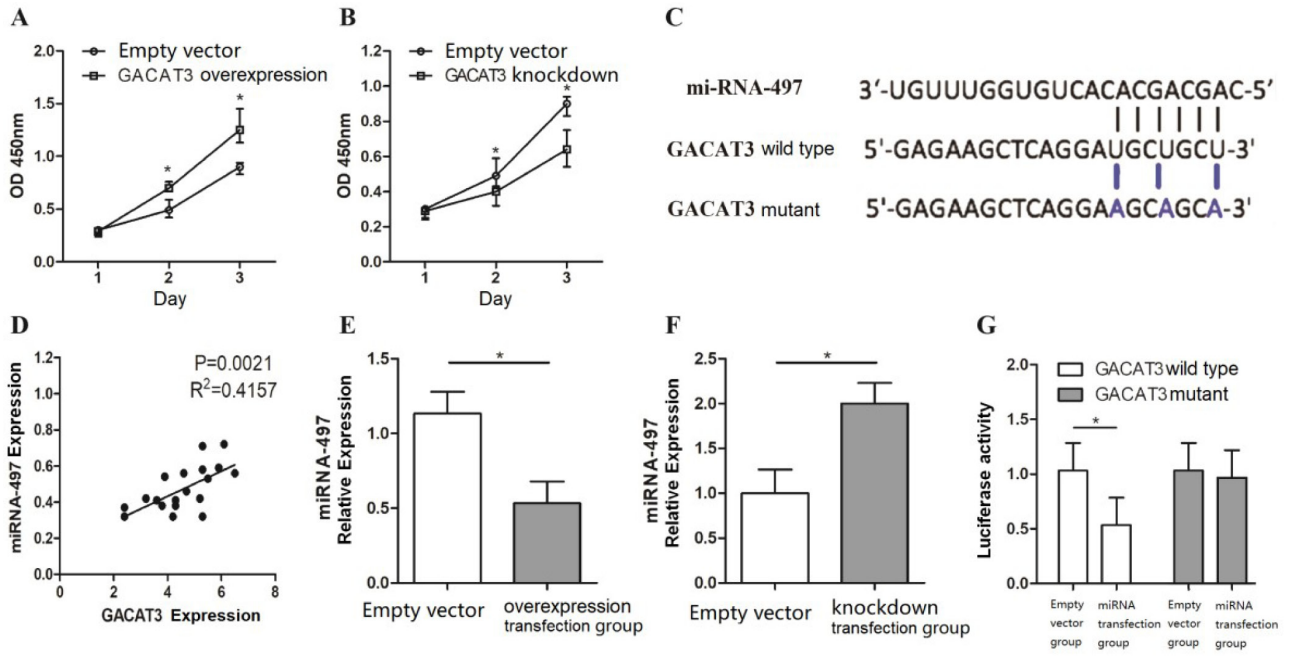

Figure 2. miR-497 is the target of LncRNA GACAT3 in the regulation of breast cancer cell proliferation. **A:** Cell proliferation in MCF-7 cells after LncRNAGACAT3 overexpression. **B:** Cell proliferation in LncRNAGACAT3 knockdown MCF-7 cells. **C:** Predicted binding sites of miR-497 in LncRNAGACAT3 (GACAT3-wild type) and GACAT3 mutant (GACAT3-MUT) sequences. **D:** Correlation analysis of the relationship between LncRNAGACAT3 and miR-497. **E:** miR-497 expression in MCF-7 cells after LncRNAGACAT3 overexpression. **F:** miR-497 expression in LncRNAGACAT3 knockdown MCF-7 cells. **G:** Luciferase activity determined in cells co-transfected with miR-497 mimics or NC mimics and pGL3 luciferase reporter containing GACAT3-WT or GACAT3-MUT sequences. *P<0.05 compared to the control.

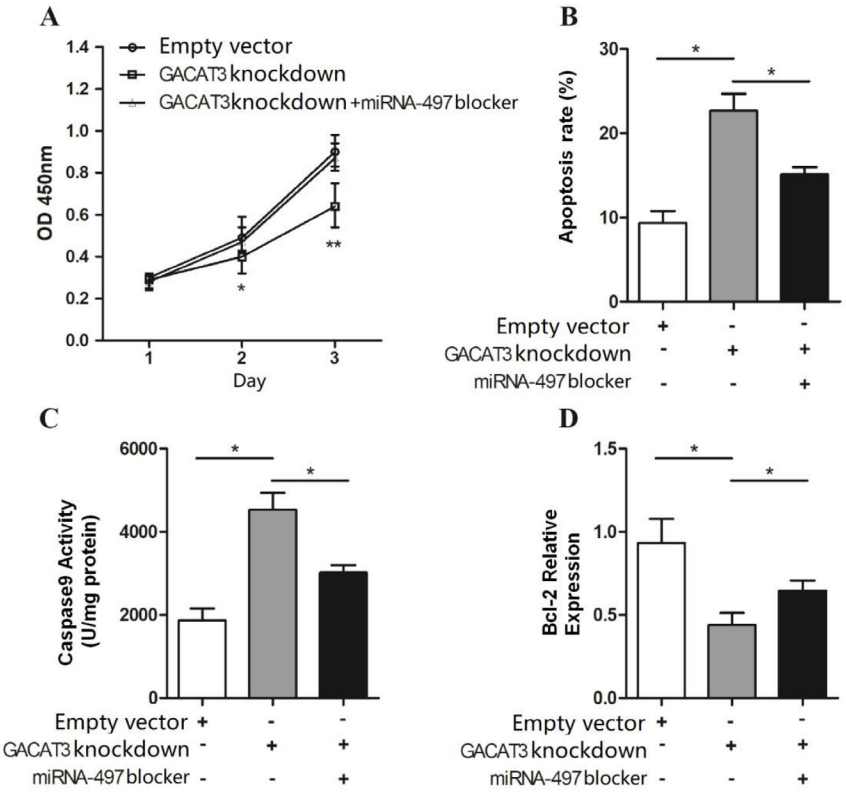

Figure 3. Knockdown of LncRNAGACAT3 leads to up-regulation of miR-497 expression and inhibition of breast cancer cell proliferation. **A:** Cell proliferation of LncRNAGACAT3 knockdown MCF-7 cells in the presence of miR-497 blocker. **B:** Apoptosis of LncRNAGACAT3 knockdown MCF-7 cells in the presence of miR-497 blocker. **C:** Activity of Caspase 9 in cell proliferation of LncRNAGACAT3 knockdown MCF7 cells in the presence of miR-497 blocker. **D:** Measurement of Bcl-2 expression by qRT-PCR in LncRNAGACAT knockdown MCF-7 cells in the presence of miR-497 blocker. *P<0.05 compared to the control.

cantly after miR-497 mimic nucleic acid transfection miR-497 increased expression, but LncRNA GACAT3 MUT luciferase activity did not decrease, and the difference was statistically significant (Figure 2G).

LnRNA knockdown of GACAT3 leads to up-regulation of miR-497 expression and inhibition of breast cancer cell proliferation

As shown in Figures 3A and B, LncRNA GACAT3 knockdown MCF-7 cells were more potent and less apoptotic than without using miR-497 inhibitors, the difference being statistically significant ($p<0.05$). In addition, knockdown of LncRNA GACAT3 promoted the enzymatic activity of caspase 9 and decreased the expression of Bcl-2 (Figures 3C and D). Compared with the uninhibited group, the miR-497 inhibitor reduced the activity of caspase 9 in MCF-7 cells and up-regulated the expression of Bcl-2 (Figures 3C and D), and the difference was statistically significant.

Discussion

Abnormally altered LncRNA has become a hot spot for prognostic markers and therapeutic targets [23]. LncRNA GACAT3, an aberrantly expressed oncogene, was first discovered to be involved in the development and progression of gastric cancer, including promoting proliferation, inhibiting apoptosis, and promoting metastasis [19,20,24,25]. Subsequently, Lnc RNA GACAT3 was found to be involved in the progression of glioma through miRNAs [26,27]. In addition, there is no report of the role of LncRNAGACAT3 in the development and progression of breast cancer.

In our study, we found that LncRNAGACAT3 is highly expressed in breast cancer tissues and cells. The high expression of LncRNAGACAT3 in breast cancer tissues indicates a poor prognosis. Not only that, but as an important means of preoperative evaluation of breast cancer, the decrease of the characteristic parameter D value and the increase of F value in NMR are considered to be indicators of poor biological behavior of the tumor and poor chemotherapy effect. This study shows that these indicators are associated with high expression of LncRNAGACAT3. This indicates that high expression of LncRNAGACAT3 is even associated with adjuvant chemotherapy tolerance after breast cancer surgery.

In addition, we investigated the role of LncRNAGACAT3 and miR-497 in breast cancer malignancies. Competing endogenous RNAs (ceRNAs) are RNA transcripts that interact at the post-transcriptional level through competitively shared miRNAs [28,29]. A large body of evidence suggests that LncRNA can serve as a ceRNA for target mRNA, possibly representing a broad form of post-transcriptional regulation of gene expression in physiology and pathology [28,29]. Whether LncRNAGACAT3 acts as a ceRNA is unclear, but the results of this study indicate that LncRNAGACAT3 may play a carcinogenic role in breast cancer as a miR-497 ceRNA. The LncRNAGACAT3miR-497 regulatory axis has rarely been reported in cancer. The role of LncRNAGACAT3 in colorectal cancer is achieved by interaction with miR-149 [25]. In the progression of glioma, miR-135 and miR-3127-5p are targets of LncRNAGACAT3 to promote tumorigenesis [26,27]. Studies have confirmed that LncRNAGACAT3 can affect the progression of gastric cancer by negatively regulating the level of miR-497 [20]. This study not only used bioinformatics to predict the relationship between LncRNAGACAT3 and miR-497 in the presence of breast cancer, but also confirmed the negative correlation in expression by qPCR and correlation analysis. Finally, the direct interaction through complementary binding sites were confirmed by dual luciferase report assay.

In different tumor studies, miR-497 targets different effector molecules to regulate tumor development [30-34]. In this study, we confirmed the inhibitory effect of miR497 in breast cancer, and this inhibition is caused by Caspase 9 and Bcl-2. Studies on the relationship between miR-497 and proliferation and apoptosis have found that miR497/Caspase 9/Bcl-2 are present in non-small cell lung cancer and glioma [35,36]. However, studies on the relationship between LncRNAGACAT3 and miR-497 involved in the regulation of Caspase 9/Bcl-2 in tumors and even diseases are still rare.

A growing number of studies have shown that LncRNA and mRNA integration network reconstruction plays an important role in the development of cancer [37]. miRNAs also play a crucial role in the regulation of cancer development and are key biomarkers for cancer diagnosis or prognosis [38]. Based on these findings, we propose that LncRNAGACAT3 and miR-497 may be useful biomarkers for predicting breast cancer progression, chemotherapy efficacy, and prognosis. Largescale clinical studies should be conducted to test the role of LncRNAGACAT3 and miR-497 in predicting breast cancer progression and prognosis.

Overall, the results suggest that LncRNAGA-

CAT3 is associated with poor prognosis, preoperative MRI perfusion-related diffusion (D) reduction, and elevated perfusion score (f) in breast cancer. Further investigation revealed that LncRNAGACAT3 acts as a regulatory RNA of miR-497, and promotes the progression of breast cancer by down-regulating Caspase 9 and up-regulating Bcl-2.

Funding

This work was funded by Qiqihar Science and Technology plan guidance project (SFZD-2017130).

Conflict of interests

The authors declare no conflict of interests.

References

1. Stagl JM, Bouchard LC, Lechner SC et al. Long-term psychological benefits of cognitive-behavioral stress management for women with breast cancer: 11 year follow-up of a randomized controlled trial. Cancer 2015;121:1873-81.
2. DeSantis C, Ma J, Bryan L, Jemal A. Breast cancer statistics, 2013. CA Cancer J Clin 2014;64:52-62.
3. Wueest S, Mueller R, Blüher M et al. Fas (CD95) expression in myeloid cells promotes obesity-induced muscle insulin resistance. EMBO Mol Med 2014;6:43-56.
4. Drukker CA, Bueno-de-Mesquita JM, Retèl VP et al. A prospective evaluation of a breast cancer prognosis signature in the observational RASTER study. Int J Cancer 2013;133:929-36.
5. Hylton NM, Blume JD, Bernreuter WK et al. Locally advanced breast cancer: MR imaging for prediction of response to neoadjuvant chemotherapy–results from ACRIN 6657/I-SPY trial. Radiology 2012;263:663-72.
6. Londero V, Bazzocchi M, Del Frate C et al. Locally advanced breast cancer: comparison of mammography, sonography and MR imaging in evaluation of residual disease in women receiving neoadjuvant chemotherapy. Eur Radiol 2004;14:1371-9.
7. Rieber A, Brambs HJ, Gabelmann A et al. Breast MRI for monitoring response of primary breast cancer to neoadjuvant chemotherapy. Eur Radiol 2002;12:1711-9.
8. Grimsby GM, Gray R, Dueck A et al. Is there concordance of invasive breast cancer pathologic tumor size with magnetic resonance imaging? Am J Surg 2009;198:500-4.
9. Le Bihan D, Breton E, Lallemand D et al. MR imaging of intravoxel incoherent motions: application to diffusion and perfusionin neurologic disorders. Radiology 1986;161:401-7.
10. Yoon JH, Lee JM, Yu MH et al. Evaluation of hepatic focal lesions using diffusion-weighted MR imaging: comparison of apparent diffusion coefficient and intravoxel incoherent motion-derived parameters. J Magn Reson Imaging 2014;39:276-85.
11. Liu C, Liang C, Liu Z et al. Intravoxel incoherent motion (IVIM) in evaluation of breast lesions: comparison with conventional DWI. Eur J Radiol 2013;82:e782-e9.
12. Gaing B, Sigmund EE, Huang WC et al. Subtype differentiation of renal tumors using voxel-based histogram analysis of intravoxel incoherent motion parameters. Invest Radiol 2015;50:144-52.
13. Kapranov P, Cheng J, Dike S et al. RNA maps reveal new RNA classes and a possible function for pervasive transcription. Science 2007;316:1484-8.
14. Batista PJ, Chang HY. Long noncoding RNAs: Cellular address codes in development and disease. Cell 2013;152:1298-1307.
15. Spizzo R, Almeida MI, Colombatti A, Calin GA. Long non-coding RNAs and cancer: A new frontier of translational research? Oncogene 2012;31:4577-87.
16. Fatica A, Bozzoni I. Long non-coding RNAs: New players in cell differentiation and development. Nat Rev Genet 2014;15:7-21.
17. Liu D, Yu X, Wang S et al. The gain and loss of long noncoding RNA associated competing endogenous RNAs in prostate cancer. Oncotarget 2016;7:57228-38.
18. Chen S, Li P, Xiao B, Guo J. Long noncoding RNA HM lincRNA717 and AC130710 have been officially named as gastric cancer associated transcript 2 (GACAT2) and GACAT3, respectively. Tumor Biol 2014;35:8351-2.
19. Shen W, Yuan Y1, Zhao M et al. Novel long non-coding RNA GACAT3 promotes gastric cancer cell proliferation through the IL-6/ STAT3 signaling pathway. Tumor Biol 2016;37:14895-902.
20. Feng L, Zhu Y, Zhang Y, Rao M. LncRNA GACAT3 promotes gastric cancer progression by negatively regulating miR-497 expression. Biomed Pharmacother 2017;97:136-42.
21. Ma L, Bajic VB, Zhang Z. On the classification of long non-coding RNAs. RNA Biol 2013;10:925-33.
22. Lin Y, Li J, Ye S et al. LncRNA GACAT3 acts as a competing endogenous RNA of HMGA1 and alleviates cucurbitacin B-induced apoptosis of gastric cancer cells. Gene 2018;678:164-71.
23. Zhou W, Wang L, Miao Y, Xing R. Novel long noncoding RNA GACAT3 promotes colorectal cancer cell proliferation, invasion, and migration through miR-149. Onco Targets Ther 2018;11:1543-52.
24. Wang J, Zhang M, Lu W. Long noncoding RNA GACAT3 promotes glioma progression by sponging miR-135a. J Cell Physiol 2019;234:10877-87.
25. Pan B, Zhao M, Xu L. Long noncoding RNA gastric cancer-associated transcript 3 plays oncogenic roles in glioma through sponging miR-3127-5p. J Cell Physiol 2019;234:8825-33.
26. Qi X, Zhang DH, Wu N, Xiao JH, Wang X, Ma W. CeRNA

in cancer: Possible functions and clinical implications, J Med Genet 2015;52:710-8.

27. Ergun S, Oztuzcu S. Oncocers: CeRNA-mediated crosstalk by sponging miRNAs in oncogenic pathways. Tumor Biol 2015;36:3129-36.
28. Li J, Zhang Y, Wang X, Zhao R. MicroRNA-497 overexpression decreases proliferation, migration and invasion of human retinoblastoma cells via targeting vascular endothelial growth factor A. Oncol Lett 2017;13:5021-7.
29. Pengcheng S, Ziqi W1, Luyao Y et al. MicroRNA-497 suppresses renal cell carcinoma by targeting VEGFR-2 in ACHN cells. Biosci Rep 2017;37.
30. Wei Z, Hu X, Liu J, Zhu W, Zhan X, Sun S. MicroRNA-497 upregulation inhibits cell invasion and metastasis in T24 and BIU-87 bladder cancer cells. Mol Med Rep 2017;16:2055-60.
31. Xu Y, Chen J, Gao C et al. MicroRNA-497 inhibits tumor growth through targeting insulin receptor substrate 1 in colorectal cancer. Oncol Lett 2017;14:6379-86.
32. Wang P, Meng X, Huang Y et al. MicroRNA- 497 inhibits thyroid cancer tumor growth and invasion by suppressing BDNF. Oncotarget 2017;8:2825-34.
33. Qin S, Zhao Y, Lim G, Lin H, Zhang X, Zhang X. Circular RNA PVT1 acts as a competing endogenous RNA for miR-497 in promoting non-small cell lung cancer progression. Biomed Pharmacother 2018;111:244-50.
34. Zhu D, Tu M, Zeng B et al. Up-regulation of miR-497 confers resistance to temozolomide in human glioma cells by targeting mTOR/Bcl-2. Cancer Med 2017;6:452-62.
35. Benador IY, Veliova M, Mahdaviani K et al. Mitochondria Bound to Lipid Droplets Have Unique Bioenergetics, Composition, and Dynamics that Support Lipid Droplet Expansion. Cell Metab 2018;27:869-85.
36. Adhami M, Haghdoost AA, Sadeghi B, Malekpour Afshar R. Candidate miRNAs in human breast cancer biomarkers: A systematic review. Breast Cancer 2018;25:198-205.
37. Benador IY, Veliova M, Mahdaviani K et al. Mitochondria Bound to Lipid Droplets Have Unique Bioenergetics, Composition, and Dynamics that Support Lipid Droplet Expansion. Cell Metab 2018;27:869-85.
38. Adhami M, Haghdoost AA, Sadeghi B, Malekpour Afshar R. Candidate miRNAs in human breast cancer biomarkers: A systematic review. Breast Cancer 2018;25:198-205.